Gravitationally Polarized Protons in Interstellar Hydrogen Gas and Dark Matter Generation

F. C. Hoh [a*#]

[a] *Dragarbrunnsg. 55C, 75320 Uppsala, Sweden.*

Original Research Article

ABSTRACT

Aims: The main purpose is to demonstrate theoretically that the *uu* diquark to *d* quark axis in a free hydrogen atom is aligned in the direction of the ambient gravitational field.
Methodology: This work is an extension of the scalar strong interaction hadron theory SSI to include gravitation.
Results: It is shown that the distance vector between the *uu* diquark and the *d* quark in a free hydrogen atom is polarized in the direction of the surrounding gravitational field with the diquark closer to the source of gravitation. This polarization of the proton is due to that the gravitational correction to the potential experienced by the diquark is four times that by the quark. It can be destroyed when the associated hydrogen atom suffers a collision in cold, interstellar hydrogen gas. But such an alignment is restored almost immediately and persists for years until another collision takes place. Dark matter is generated and persists in the meantime if the gas has a gradient along the gravitational field. In the derivation, new insights in quark dynamics are uncovered and explained. The sum of the quark masses is about twice the proton mass so the quarks are strongly bond. The strong interaction strength between the *u* and *d* quarks in nucleon is nearly the same as that between a quark and an antiquark in meson.

_____

[#] *Retired;*
Corresponding author: E-mail: hoh@telia.com;

Conclusion: Cold interstellar hydrogen gas in gravitational field can generate dark matter and dark energy which however disappear when the gas becomes hot and dense or is converted into star or planet.

1. INTRODUCTION

The current official theory of elementary particles, the standard model SM [1,2], cannot explain hadron data and the presence of dark matter and dark energy. The scalar strong interaction hadron theory SSI [3,4] has been more successful in accounting for such data. Recently, dark matter and dark energy were recognized to be inherent in SSI which could be extended to account for many such dark phenomena [5-8]. Such findings have been mentioned in the introduction of [8].

These findings have been based upon the heuristic assumption that the *uu* diquark and the *d* quark in ground state proton in cold, tenuous hydrogen gas are polarized in the direction of the ambient gravitational field emanating from a large mass, e. g., the center of a galaxy, with the heavier diquark lying closer to such a center, as is reflected in Fig. 1.

Applications of SSI in e. g. Fig. 1 of [8], Figures. 2-3 of [7] and Figs. 2-4 of [6] for generation of dark matter and the equivalent of dark energy and for removal of gravitational singularity are all based upon this polarization of proton. Therefore, it is of interest to demonstrate the correctness of this heuristic assumption theoretically.
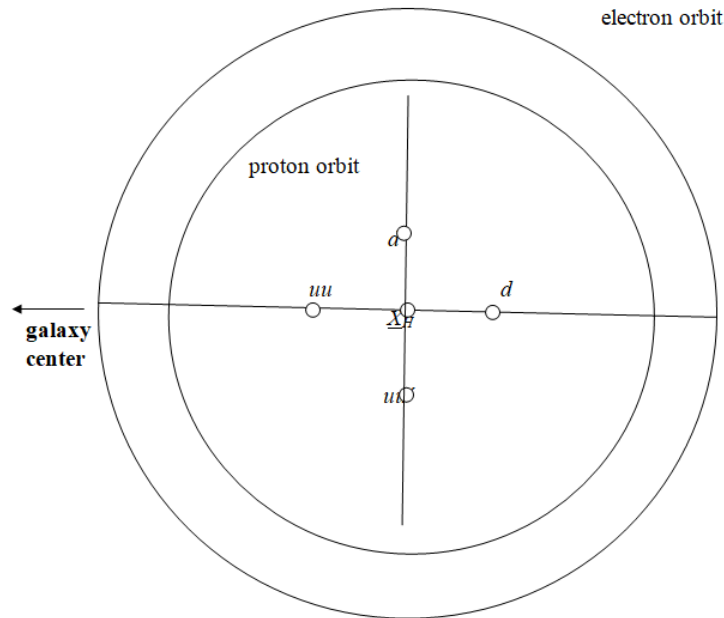

Fig. 1. Schematic structure of a free, test hydrogen atom in SSI. The large electron orbit has been scaled down to fit inside this figure. $\underline{X}_H$ denotes the coordinate of the center of this test atom. It is also the center $\underline{X}_e$ of the electron charge cloud having a radius of 0.53Å (Bohr radius a_0, outer circle) as well as the center $\underline{X}_p$ of the proton charge cloud having a radius of 28.8 fm (proton Bohr radius a_{0p}, inner circle). The small distance $r = |\underline{x}|$ between the *uu´* (or *uu*) diquark and the *d´* (or *d*) quark has been scaled up for illustration. In the absence of gravitational field, $\underline{x}$ can form any angle with the horizontal axis. Here, the angles 0° for *uu-d* and 270° for *uu´-d´* have been chosen for illustration. When a gravitational field is present, as is indicated by the left arrow towards a galaxy center, the vector $\underline{x}$ will align itself along direction of this field. The quarks will now lie on the horizontal axis with heavier *uu* diquark closer to the galaxy center

Actually, this assumption does not follow from classical mechanics. In Fig. 1, let the *uu´-d´* pair be point particles in Newtonian mechanics. The gravitational forces on the diquark *uu´* and quark *d´* are proportional to their respective masses according to (A2). Follow Newton's law and equate these forces to mass×acceleration for the *uu´* and *d´* particles, respectively, the mass of each of the speicies cancel out. This leads to that both *uu´* and *d´* experience the same acceleration. In this case, turning on the gravitational field will move *uu´* and *d´* towards the left as a unit and will not lead to the polarized *uu-d* configuration in Fig. 1.

But the *uu´-d´* quarks are not classical particles in the present quantum-mechanical SSI. The main purpose of this paper is to show such polarization of the proton in a free hydrogen atom caused by the ambient gravitational field starting from the basic equations of motion of quarks in SSI, extended to include gravitation, and thereby justify of the above heuristic assumption. In this process, new insights of SSI are uncovered and presented.

For reference, some relevant parts and extensions of SSI are reproduced in the appendices.

2. GRAVITATIONAL POLARIZATION OF QUARKS IN HYDROGEN ATOM AND DARK MATTER

The parameter regions in the present investigation will be taken to be those pertaining to the Milky Way. The interstellar medium in it is dominated by rarified, cold hydrogen atoms with a density of 20-50 atoms/cm^3 and a temperature of 50-100 °K. Let the collision crossection between two such atoms be the hard sphere disk of $4\pi a_0^2$. In this medium, the magnitude of the mean free path of a test hydrogen atom is 10 AU and of the mean collision time 10 years. Thus, such a hydrogen atom is free and can generate dark matter or dark energy that persist except for a negligibly short time after a collision (see §2.2 below).

Note that in stars and planets, the hydrogen atoms interact frequently with other particles and are not free like those in the interstellar medium and eventual dark matter generated cannot persist.

Let the atom with *uu-d* in Fig. 1 be a test atom in this interstellar medium. The *uu-d* quarks experience interquark strong confining force and the gravitational force from the galaxy center. In a collision, two atoms interact electromagnetically via their electrons. The accompanying force is transmitted to the proton via Coulomb interaction so that the quarks are eventually also affected by this force.

In Fig. 2, collision of the test atom in Fig. 1 with another atom causes the *d-uu* quark aggregate, originally located along the horizontal axis, to move to a new position denoted by *d´´-uu´´* having the same interquark distance (see rigid "*d-uu* rod" in §**A8**). In quasi-steady state, *uu´´*, *d´´* and the proton at $\underline{X}_p$ all lie on a straight line, as they did before the collision on the horizontal line, according to (A16) which can be written as

$$a_m = \frac{X^\mu - x_I^\mu}{x_{II}^\mu - x_I^\mu} = \frac{X^0 - x_I^0}{x^0} = \frac{\underline{X} - x_I}{\underline{x}}$$

1

where $\underline{X}$ stands for $\underline{X}_p$.

2.1 Gravitational Polarization of Proton in Hydrogen Atom

Equations of motion for the diquark *uu´´* in Fig. 2 given by (A10) is written in the form

$$\partial_I^{ab}\partial_I^{gh}\chi_{A\{b\dot{h}\}}(x_I) = -\left(V_{AB}^2(x_I)(1+\Lambda_{Guu}(x_I))+m_A^2\right)\psi_A^{\{ag\}}(x_I)$$

$$\partial_{I\,b\dot{c}}\partial_{I\,hk}\psi_{A\{b\dot{h}\}}(x_I) = -\left(V_{AB}^2(x_I)(1+\Lambda_{Guu}(x_I))+m_A^2\right)\chi_{A\{b\dot{h}\}}$$

2

$$\Lambda_{Guu}(x_I) = 2V_{AG}(x_I)/V_{AB}(x_I)$$

3

Similarly, the quark equations (A11) for quark *d´´* in Fig. 2 becomes

$$\partial_{II}^{d\dot{e}}\chi_{B\dot{e}}(x_{II}) = i\left(2V_{BA}(x_{II})(1+\Lambda_{Gd}(x_{II}))+m_B\right)\psi_B^d(x_{II})$$

$$\partial_{II\,\dot{e}f}\psi_B^f(x_{II}) = i\left(2V_{BA}(x_{II})(1+\Lambda_{Gd}(x_{II}))+m_B\right)\chi_{B\dot{e}}(x_{II})$$

4

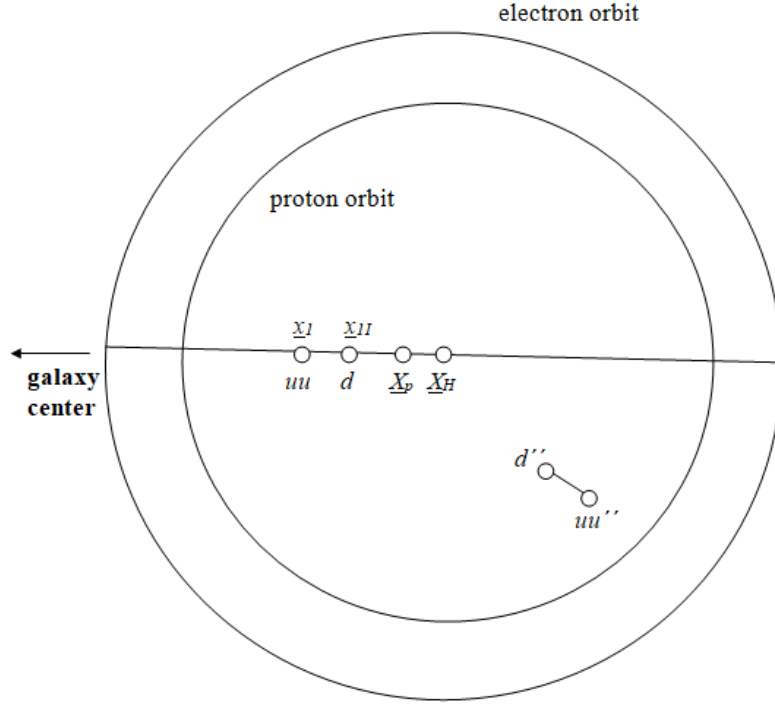$$\Lambda_{Gd}(x_{II}) = V_{BG}(x_{II})/2V_{BA}(x_{II})$$

5

Fig. 2. Schematic structure of the test hydrogen atom in Figure 1 before and after a collision with another hydrogen atom in interstellar medium. The *uu-d* quarks before the collision have been moved to the positions denoted by *uu´´-d˝*

Here, Δ_{Guu} represents the correction to the potential experienced by the diquark *uu´´* due to the presence of gravitation. Analogously, Δ_{Gd} represents the corresponding correction for the quark *d´´*.

With (A22), (A21) and (A2), these corrections can be written in the form

$$\Lambda_{Guu}(x_I) = \left(-\frac{GM_g}{|\underline{x}_I|} m_A \right) \left(\frac{2}{V_s(r)} \right)$$

5

$$\Lambda_{Gd}(x_{II}) = \left(-\frac{GM_g}{|\underline{x}_{II}|} m_B \right) \left(\frac{1}{2V_s(r)} \right)$$

6

Since the *u* quark mass $m_A \cong m_B$, the *d* quark mass, and $|\underline{x}_{II}| \cong |\underline{x}_I|$, these results show that the gravitational correction Δ_{Guu} of the potential experienced by the diquark *uu´´* is four times greater than Δ_{Gd} for the *d´´* quark. Since the gravitational force acting on these quarks are gradients of these potentials, the *uu´´* diquark

experiences a gravitational pulling force four times that by the *d´´* quark.

Putting this force equal to mass×acceleration, the acceleration towards the galaxy center experienced by the diquark *uu´´* is twice that experienced by the quark *d´´*. This situation differs from the classical mechanics model mentioned below Fig. 1 in which *uu´* and *d´* experience the same acceleration. Therefore, the diquark *uu´´* will move towards the galactic center faster than the *d´´* quark does in Fig. 2. The *d´´-uu´´* rod will be polarized by the gravitational field and return to an orientation same as that before the collision, i. e., that of the *d-uu* rod in Fig. 2.

2.2 Estimate of Relaxation Time

The *uu´´-d´´* distance is the same as the *d-uu* rod length $r_a \approx 3.05$ fm, mentioned in §A8 and fixed by the strong interquark potential V_s in (A22), shown in Fig. A1. Gravitational force cannot change this length but can change the orientation of this *uu´´-d´´* rod to that before the collision.

The time scale needed for such a change may be estimated quasi-classically as follows. In §2.1,

the relative gravitational acceleration $\underline{a}_r$ between uu'' and d'' is seen to be the same as the acceleration $\underline{a}_{BG}$ of the d'' quark. It can be estimated from (A2);

$$\underline{a}_r\left(\underline{x}_{II}\right) \approx \underline{a}_{BG}\left(\underline{x}_{II}\right) = -\frac{\partial V_{BG}\left(\underline{x}_{II}\right)}{m_B \partial \underline{x}_{II}} = -\frac{GM_g}{|\underline{x}_{II}|^2} \approx 1.48 \times 10^{-10}\ \text{m/s}^2$$

7

where the Milky Way mass $M_g \approx 10^{12} \times M_{SUN}$ and the galaxy radius $|\underline{x}_{II}| \approx 100$ kly(kilo light years).

This relative acceleration $\underline{a}_r$ is directed towards left and is parallel to the horizontal axis in Fig. 2. It can be split up in a component $\underline{a}_{r1}$ parallel to $\underline{x}$ and a component $\underline{a}_{r2}$ perpendicular to it. $\underline{a}_{r1}$ will push this d''-uu'' rod towards left and upwards along $\underline{x}$. $\underline{a}_{r2}$ will tend to swing uu'' downwards towards the left in a circular movement and cause it to pass d'' until it ends up on its left side on a horizontal line. The original d-uu rod configuration is recovered.

The distance covered by this movement is of the magnitude $\pi r_a \approx 9.6$ fm. Let the component $\underline{a}_{r2}$ be approximated by $\underline{a}_r/2$ which covers a distance of the magnitude of $a_r t_c^2/4$ where t_c is the time from collision. Equating these two distances provides an estimate of $t_c \approx 0.04$ s. This time is negligible next to the mean collision time of 10 years mentioned above Fig. 1.

Thus, the d''-uu'' rod will "immediately" after the collision change its orientation back to the original one and end up in the polarized configuration with uu lying closer to the mass center of the galaxy, like the original d-uu rod in Fig. 2.

2.3 Gas Pressure Gradient and Dark Matter Generation

Due to the higher gas pressure near the galaxy center, the interstellar gas is expanding. The test hydrogen atom in Fig. 2 collided with another atom. The collision is largely of Coulomb nature and will on the average push the electron of the test atom outwards away from the galaxy center leaving its proton and the quarks behind at first. The proton and quark coordinates $\underline{X}_p$, $\underline{x}_I$ and $\underline{x}_{II}$ all lie to the left of the center $\underline{X}_H$ of the test atom. In this configuration, $a_m > 0$ in (1) gives rise to negative relative energy $-\omega < 0$ or dark matter shown in §A7 below.

In §A7, the upper limit of the ratio $|R_{DM}|$ of the so-generated dark matter to the ordinary matter that generates it is 8.94. The observed ratio $|R_{DM}| \approx 5$ [1 dark matter] lies between this value and 0.

2.4 Differential Gravitational Pull

Table 5.2 of [4] gives the u and d quark masses $m_u = 659.2$ MeV and $m_d = m_u + 2.15$ MeV. The mass of the uu-d rod is thus greater than twice the proton mass 938.3 MeV. The uu and d positions $\underline{x}_I$ and $\underline{x}_{II}$ will tend to be pulled by gravitation to the left of the proton position $\underline{X}_p$ in Fig. 2. This tends to reinforce or maintain the dark matter generated by collisions in the gas pressure gradient environment in §2.3.

3. DISCUSSION RELATED TO THE RESULTS

The results of Section 2 removes the heuristic assumption of gravitational polarization of proton in Section 1 upon which the earlier papers [5-8] were based. This required polarization of the uu-d quarks in the test atom in Fig. 2 can been derived from the basic equations of motion of quarks in gravitational field.

As the extension to include gravitation in SSI takes place at the very basic, starting level, light has been shed on several features in SSI of basic interest.

3.1 Application to the Expanding Universe

In current view, the universe expanded during the first half of its life during which it had a large pressure gradient near its center and dark matter prevailed. This scenario is similar to that in §2.3 where the dark matter to ordinary matter ratio $|R_{DM}|$ of (A29) may reach up to its maximum value of ~ 9. Dark energy was absent.

As the universe and galaxies expand, they cool down, particularly in their outskirts where the hydrogen gas pressure is low and its gradient small. In those regions, the electrons in in Fig. 2 is no longer pushed to the right by collisions and the uu-d quarks on left side in Fig. 2 move back to the neutral position in the center of the test atom as in Fig. 1 where $|R_{DM}| = 0$. The mechanisms of §2.3 are eventually replaced by the mechanism of [8 §3]. Some of the centers of the uu-d quarks will enter the right half of Fig. 2. This will give rise to positive relative energy

(PRE) identified as dark energy here. The numbers of such atoms are fewer than those producing dark matter but their energies can increase uninhibitedly and become "run away" hydrogen atoms moving away from the mass center of the universe with acceleration [8 §3,4].

These features also agree with the current view that dark energy appeared long after the dark matter, are present only in regions with low hydrogen gas density and temperature and account for the accelerating expansion of the universe.

3.2 Filament Formation [8 §2.3]

In recent decades, a large part of the universe has been found to consist of "filaments" or thread-like structures forming networks rather than homogeneous gas clouds. This may also be accounted for by the mechanism of §2.3.

Consider a cylinder of tenuous, cold hydrogen gas cloud. The gas near the cylinder surface will fall towards the cylinder axis. An atom in this gas will according to the configuration on the left side of Fig. 2, where the galaxy center is replaced by the cylinder axis, produce dark matter which tends to increase the fall speed. The gas along the cylinder axis will not produce any dark matter due to symmetry but will be compressed by the falling matter and dark matter and produce a radial pressure gradient like that in §2.3. This cylinder then shrinks into a thin cylinder or a "filament" consisting mostly of dark matter except for its core which now contains hydrogen gas with high density. Stars or eventually galaxies may be formed along this matter and dark matter filament. The observed ratio of dark matter/visible matter of about 5 in such filaments is compatible with the upper limit of $|R_{DM}| < 8.94$ in (A29).

3.3 Dark Matter Behavior

The so-generated dark matter is attached to the proton that generates it. It simply increases the proton mass E_0 by a factor of $1+|R_{DM}|$ gravitationally. This proton retains E_0 in electromagnetic interactions, which takes place only in the observable laboratory space X^μ in (A16). On the other hand, gravitational potential, being scalar at such low energies, enters the equations of motion of quarks next to the strong, scalar quark-quark potential in e. g. (A1). These potentials depend upon the quark coordinate $x_{\parallel}$ which contains the "hidden" space x^μ as well as the observable space X^μ in (A16). Parts of these quantities associated with x^μ is thus unobservable or "dark".

In (A1), gravitation is naturally integrated with the quark motion in the quantum-mechanical SSI.

Dark matter in a galaxy can thus in principle account for the galaxy's rotation curve [6 §8]. Star and planet formation in a galaxy uses up its hydrogen atoms and thereby reduces its dark matter content.

Protons that generate dark matter have gravitational mass $(1+|R_{DM}|)E_0$ and will interact with each other with this enhanced mass. This may be supported by the recent observation that dark matter interact with each other in colliding galaxies.

3.4 Confinemet

Confinement of quarks in SSI arises naturally from the harmonic potentials $\propto r^2$ in Φ_b of (A24) for baryons and in Φ_m of (A27) for mesons. Such a dependence is a consequence of the higher order nature of the interquark potential equations (A23) and [4 (3.1.11)] which has the same form; $\Delta\Delta = (\partial/\partial \underline{x})^4$ in them allows for a confining solution $\propto r^2$. Such a potential is absent in the standard model in which confinement is also not proven.

As Φ_b and Φ_m have different dimensions, the r^2 terms in them cannot be compared directly. But the u-d interaction potentials V_s in (A22) and V_{sm} in (A28) derived from them can. These potentials should have about the same strength in meson and nucleon. This turns out to be the case, as is mentioned beneath (A28). Such strong interaction potential is of the order of magnitude of GeV, about 10^5 times stronger than the electromagnetic interactions in atoms.

The quark masses in §2.4 are about twice that of the conventional constitutional quark mass ~315 MeV obtained from e. g. baryon magnetic moments considerations. In the last case, the quark mass contribution to the proton mass is ~945 MeV, barely exceeding the proton mass. The binding energy is then ~7 MeV which appears to be too small; the quarks may, according to conventional quantum mechanics, eventually escape if the proton suffers a collision, contrary to experience.

The large quark masses here, on the other hand, leads to a binding energy (A24) greater than the

proton mass itself; quarks are strongly bound and can hardly escape. Due to the small pion mass, the quarks in pions are bound even harder by the large constant d_{m0} in (A27). Besides, there are no free quarks in SSI.

4. CONCLUSION

From the equations of motion of quarks in the scalar strong interaction hadron theory SSI, extended to include gravitation, quarks in cold, rarified hydrogen gas with pressure gradient can be polarized by the ambient gravitational field. This polarization together with atomic collisions in the gas leads to dark matter generation compatible with that observed. Such effects vanish when the gas becomes hot and dense.

COMPETING INTERESTS

Author has declared that no competing interests exist.

REFERENCES

1. Wikipedia. Standard model; 2021. Available:https://en.wikipedia.org/wiki/Main _Page
2. Burgess C, Moore G, The standard model, a primer. Cambridge; 2007
3. Hoh FC. Spinor strong interaction model for baryon spectra. Int. J. Theoretical Physics. 1994;33 2325-49.
4. Hoh FC. Scalar strong interaction hadron theory II, New York: Nova Science; 2019.
5. Hoh FC. Dark energy and dark matter as relative energy between quarks in nucleon. J. Modern Physics. 2019;10:635-40. Available:https://doi.org/10.4236/jmp.2019. 106045
6. Hoh FC. Cosmic applications of relative energy between quarks in nucleons. J. Modern Physics. 2019;10:1645-58. Available:https://doi.org/10.4236/jmp.2019. 1014108
7. Hoh FC. On the ratio dark matter(energy)/ordinary matter $\approx$ 5.4(13.6)in the universe. J. Modern Physics. 2020;11:967-75. Available:https://doi.org/10.4236/jmp.2020. 117060
8. Hoh FC. Dark matter creation and anti-gravity acceleration of the expanding universe. J. Modern Physics. 2021;12:139-160. Available:https://doi.10.4236/jmp.2021.123 013
9. Lichtenberg DB. Energy levels of quarkonia in Potential models. Int. J. Modern Physics.1987;2:1669-1705.

APPENDICES. SSI EXTENDED TO APPLY TO NUCLEON IN GRAVITATIONAL FIELD

Some basic SSI equations underlying the above treatment are reproduced for reference. This appendix differs from that in [7] where the gravitational potentials were grouped together which the quark masses in order to show how they effectively modify these masses. Here, these potentials are group together with the strong, interquark potentials in order to show how they effectively modify the motion of the quarks.

In this process, some basic properties of the strong interaction interquark potentials are seen explicitly, notably in §**A6** and §**A8.** These bonding potentials are of the same magnitude in both mesons and nucleons. The quarks are naturally confined by harmonic potentials. The sum of the proton's three quark masses is about twice the proton mass; the difference is of the magnitude of such strong bonding potentials.

A1 Equations of motion for quarks in gravitational field

In SSI, the equations of motion of baryon are constructed from the equations of motion of three quarks A, B and C located at x_I, x_{II} and x_{III}, respectively, given by [4 (9.1.1-4)]. When gravitation is taken into account, an extra gravitational potential is added to these equations. Thus, (9.1.2) of [4] for quark B becomes (2.1) of [6]

$$\partial_{II}^{d\dot{e}}\chi_{B\dot{e}}(x_{II}) - i(V_{BC}(x_{II}) + V_{BA}(x_{II}) + V_{BG}(x_{II}))\psi_B^d(x_{II}) = im_B\psi_B^d(x_{II})$$
$$\partial_{II\,\dot{e}f}\psi_B^f(x_{II}) - i(V_{BC}(x_{II}) + V_{BA}(x_{II}) + V_{BG}(x_{II}))\chi_{B\dot{e}}(x_{II}) = im_B\chi_{B\dot{e}}(x_{II})$$

A1

where $\partial_{II} = \partial/\partial x_I$ and m_B is the mass of quark B. χ_B and ψ_B are quark spinors which are linear combinations of the four components in the conventional Dirac bispinor ψ [4 (C11)]. The spinor indices run from 1 to 2. $V_{BA}(x_{II})$ stands for the strong scalar potential at x_{II} generated by quark A at x_I and $V_{BC}(x_{II})$ for that generated by quark C at x_{III}. V_{BG} is an external gravitational potential experienced by quark B and has the form (A1) of [7],

$$V_{BG}(x_{II}) = m_B\varepsilon_{II}, \qquad \varepsilon_{II} = \varepsilon_{II}(|\underline{x}_{II}|) = -\frac{GM_g}{|\underline{x}_{II}|}$$

A2

Here, G is the gravitational constant. Taking the Milky Way as an example, M_g is its mass and $\underline{x}_{II}$ the distance vector between the center of this mass and quark B and may be of the magnitude of 100 lyr. ε_{II} is thus a small number of the magnitude of $!0^{-6}$ and V_{BG} is a perturbative gravitational potential.

The equations of motion for quarks A and C (9.1.1, 3) of [4] have similarly been extended to include gravitation to arrive at (A3) and (A4) of [7], which takes the following form here,

$$\partial_I^{a\dot{b}}\chi_{A\dot{b}}(x_I) - i(V_{AB}(x_I) + V_{AC}(x_I) + V_{AG}(x_I))\psi_A^a(x_I) = im_A\psi_A^a(x_I)$$
$$\partial_{I\,\dot{b}c}\psi_A^c(x_I) - i(V_{AB}(x_I) + V_{AC}(x_I) + V_{AG}(x_I))\chi_{A\dot{b}}(x_I) = im_A\chi_{A\dot{b}}(x_I)$$

A3

$$\partial_{III}^{g\dot{h}}\chi_{C\dot{h}}(x_{III}) - i(V_{CA}(x_{III}) + V_{CB}(x_{III}) + V_{CG}(x_{III}))\psi_C^g(x_{III}) = im_C\psi_C^g(x_{III})$$
$$\partial_{III\,\dot{h}k}\psi_C^k(x_{III}) - i(V_{CA}(x_{III}) + V_{CB}(x_{III}) + V_{CG}(x_{III}))\chi_{C\dot{h}}(x_{III}) = im_C\chi_{C\dot{h}}(x_{III})$$

A4

A2 Construction of equations of motion of diquark

Follow the procedure of (A5) and (A6) of [7], multiply (A3) by (A4) and generalize the product wave functions into nonseparable diquark wave functions like those in (2.2.2-3) of [4]. The result reads.

$$\chi_{A\dot{b}}(x_I)\chi_{C\dot{h}}(x_{III}) \rightarrow \chi_{AC\{\dot{b}\dot{h}\}}(x_I, x_{III}), \quad \psi_A^c(x_I)\psi_C^k(x_{III}) \rightarrow \psi_{AC}^{\{ck\}}(x_I, x_{III})$$

A5

$$V_{ABCG}^2(x_I, x_{III}) = \left(V_{AB}(x_I) + V_{AC}(x_I) + V_{AG}(x_I)\right)\left(V_{CA}(x_{III}) + V_{CB}(x_{III}) + V_{CG}(x_{III})\right)$$

A6

$$\partial_I^{a\dot{b}}\partial_{III}^{g\dot{h}}\chi_{AC\{\dot{b}\dot{h}\}}(x_I, x_{III}) = -\left(V_{ABCG}^2(x_I, x_{III}) + m_A m_C\right)\psi_{AC}^{\{ag\}}(x_I, x_{III})$$

$$\partial_{Ibc}\partial_{IIIhk}\psi_{AC\{\dot{b}\dot{h}\}}(x_I, x_{III}) = -\left(V_{ABCG}^2(x_I, x_{III}) + m_A m_C\right)\chi_{AC\{\dot{b}\dot{h}\}}(x_I, x_{III})$$

A7

In this process, mixed spinors possessing one dotted and one undotted indices transform like mesons, which are absent here, and are dropped, similar to the equivalent procedure in Sec. 9.2 of [4].

A3 Equations of motion for diquark and quark in gravitational field

Follow the procedure of (A5a) of [7] and move quark *C* at x_{III} towards quark *A* at x_I and let both quarks be merged into a diquark,

$$\chi_{AC\{\dot{b}\dot{h}\}}(x_I, x_{III}) \rightarrow \chi_{A\{\dot{b}\dot{h}\}}(x_I), \quad \psi_{AC}^{\{ck\}}(x_I, x_{III}) \rightarrow \psi_A^{\{ck\}}(x_I)$$

A8

In ground state nucleons, (A7) describes the *uu* diquark in a proton or the *dd* diquark in a neutron. The remaining quark obeys the quark equation (A1).

In this merging process, V_{AC} and V_{CA} drop out and $V_{CB}=V_{AB}$ in (A6). Since *G* in (A2) is small, only terms linear in $V_{AG}=V_{CG}$ need be included in (A6) so that

$$V_{ABCG}^2(x_I, x_{III}) \rightarrow V_{AB}^2(x_I) + 2V_{AB}(x_I)V_{AG}(x_I)$$

A9

The diquark equations (A7) now become

$$\partial_I^{a\dot{b}}\partial_I^{g\dot{h}}\chi_{A\{\dot{b}\dot{h}\}}(x_I) = -\left(V_{AB}^2(x_I) + 2V_{AB}(x_I)V_{AG}(x_I) + m_A^2\right)\psi_A^{\{ag\}}(x_I)$$

$$\partial_{Ibc}\partial_{Ihk}\psi_{A\{\dot{b}\dot{h}\}}(x_I) = -\left(V_{AB}^2(x_I) + 2V_{AB}(x_I)V_{AG}(x_I) + m_A^2\right)\chi_{A\{\dot{b}\dot{h}\}}$$

A10

The quark equations (A1) now become

$$\partial_{II}^{d\dot{e}}\chi_{B\dot{e}}(x_{II}) = i\left(2V_{BA}(x_{II}) + V_{BG}(x_{II}) + m_B\right)\psi_B^d(x_{II})$$

$$\partial_{II\dot{e}f}\psi_B^f(x_{II}) = i\left(2V_{BA}(x_{II}) + V_{BG}(x_{II}) + m_B\right)\chi_{B\dot{e}}(x_{II})$$

A11

A4 Equations of motion for nucleon

Following the steps that led to the nucleon wave equations in (A9) of [7], multiplyimg (A10) by (A11) leads analogously to

$$\partial_I^{a\dot{b}}\partial_I^{g\dot{h}}\partial_{II\dot{e}f}\chi_{\{\dot{b}\dot{h}\}}^f(x_I, x_{II}) = -i\left(m_A^2 m_B + \Phi_b(x_I, x_{II}) + \Phi_G(x_I, x_{II})\right)\psi_{\dot{e}}^{\{ag\}}(x_I, x_{II})$$

$$\partial_{Ibc}\partial_{Ihk}\partial_{II}^{d\dot{e}}\psi_{\dot{e}}^{ck}(x_I, x_{II}) = -i\left(m_A^2 m_B + \Phi_b(x_I, x_{II}) + \Phi_G(x_I, x_{II})\right)\chi_{\dot{b}\dot{h}}^d(x_I, x_{II})$$

A12

(A10) of [7] reads

$$\Box_I, \Box_I, \Box_{II} \, \Phi_b(x_I, x_{II}) = \frac{1}{4} g_s^6 \left\{ \chi_{\{bh\}}^{\ f}(x_I, x_{II}) \psi_{\ f}^{\{bh\}}(x_I, x_{II}) + c.c. \right\}$$

A13

where g_s is the strong quark-quark coupling constant,

$$\Phi_b(x_I, x_{II}) = 2V_{AB}^2(x_I) V_{BA}(x_{II})$$

A14

is the strong diquark-quark interaction potential and

$$\Phi_G(x_I, x_{II}) = 4V_{AG}(x_I) V_{AB}(x_I) V_{BA}(x_{II}) + V_{BG}(x_{II}) V_{AB}^2(x_I)$$

A15

is the correction to Φ_b in due to gravitation.

A5 Laboratory and "hidden", relative coordinates and solutions

The unobservable quark coordinates x_{II} and x_I have been transformed into a visible laboratory coordinates X and an unobservable "hidden" relative coordinate x according to (3.1.3a) of [4], also shown in (A2) of [8];

$$x^\mu = x_{II}^\mu - x_I^\mu, \quad X^\mu = (1 - a_m)x_I^\mu + a_m x_{II}^\mu, \quad a_m = (X^\mu - x_I^\mu)/(x_{II}^\mu - x_I^\mu)$$
$$x_I = X - a_m x, \quad x_{II} = X + (1 - a_m)x$$

A16

where a_m is an arbitrary real constant. The wave functions in (A12) have been decomposed into plane wave solutions according to (10.1.1) of [4] or (A3) of [8],

$$\chi_{\{bh\}}^{\ f}(x_I, x_{II}) = \chi_{\{bh\}}^{\ f}(\underline{x}) \exp(i\omega x^0) \times \exp(-iK_\mu X^\mu)$$
$$\psi_{\ \dot{e}}^{\{ag\}}(x_I, x_{II}) = \psi_{\ \dot{e}}^{\{ag\}}(\underline{x}) \exp(i\omega x^0) \times \exp(-iK_\mu X^\mu), \quad K_\mu = (E_K, -\underline{K})$$

A17

Here, E_K is the nucleon energy and $\underline{K}$ its momentum. x^0 is the relative time and $-\omega$ the relative energy between the diquark and the quark, respectively. In the following, the laboratory coordinate X^μ will be identified as the proton coordinate X_p^μ. The wave functions χ and ψ have 6 components each comprising of a spin 1/2 doublet part $\chi_{0\dot{a}}, \psi_0^a$ [4 (9.2.2)] and a spin 3/2 quartet part [4 (9.2.8)]. $-\omega < 0$ has been assigned to dark matter in [5].and $-\omega > 0$ to dark energy or PRE (positive relative energy in [8])

Consider the rest frame $\underline{K} = 0$ doublet baryons and put [4 (3.1.10a)] or [7 (2.4)],

$$a_m = 1/2 + \omega/E_0$$

A18

Putting aside gravitation for a moment, (A12) can with (A16-A18) be decomposed into a quartet part for the spin 3/2 baryons [4 (10.5.1)] and a doublet part for the spin 1/2 baryons [4 (10.2.1a)] or [8 (A5)] which reads

$$\left(i\delta^{ab}E_0/2 + \underline{\sigma}^{ab}\underline{\partial}\right)\left(E_0^2/4 + \Delta\right)\chi_{0b}(\underline{x}) = i\left(M_b^3 + \Phi_b(\underline{x})\right)\psi_0^a(\underline{x})$$

$$\left(i\delta_{bc}E_0/2 - \underline{\sigma}_{bc}\underline{\partial}\right)\left(E_0^2/4 + \Delta\right)\psi_0^c(\underline{x}) = i\left(M_b^3 + \Phi_b(\underline{x})\right)\chi_{0b}(\underline{x}), \quad \Delta = \partial^2/\partial\underline{x}^2$$

A19

$$M_b = (2m_A + m_B)/2$$

A20

In SSI, the quark masses have been replaced by mass operators operating on internal wave functions and $m_A{}^2m_B$ in (A12) are replaced by $M_b{}^3$ [4 §9.3.3].

$V_{BA}(x_{II})$ as defined above (A2) is a scalar potential describing the interaction between the u and d quarks involving the positions of the both quarks. The only scalar that can be formed here is the distance between these two quarks. By (A16), this distance is

$$r = \left|\underline{x}\right| = \left|\underline{x}_{II} - \underline{x}_I\right|$$

A21

The relative time has been put to 0 here as the quark coordinates refer to those having the same time.

Thus, the mutual interaction between the two quarks is independent of X or where they are located in the laboratory frame. Such a potential is analogous to the Coulomb or gravitational potential. Noting this and (A14), one can put

$$V_s(r) = V_{AB}(x_I) = V_{BA}(x_{II}), \quad \Phi_b(r) = \Phi_b(x_I, x_{II}) = 2V_s^3(r), \quad V_s(r) = \left(\Phi_b(r)/2\right)^{1/3}$$

A22

For the plane wave solutions in (A17), the normalized amplitudes of the wave functions with $\underline{K} = 0$ vanishes so that the right side of (A13) also drops out. With (A22), (A13) becomes

$$\Delta\Delta\Delta \; \Phi_b(r) = 0$$

A23

which has the solution [6 (4.2)] or [4 (10.2.2a)]

$$\Phi_b(r) = \frac{d_b}{r} + d_{b0} + d_{b1}r + d_{b2}r^2 + d_{b4}r^4$$

A24

where the d_b's are constants.

For the wave functions in (A19), the ansatz [4 (10.3.8a)] reads

$$\psi_0^1(\underline{x}) = \frac{1}{\sqrt{4\pi}}\left(g_0(r) + if_0(r)\cos\theta\right), \qquad \chi_{0i}(\underline{x}) = \left(\psi_0^1(\underline{x})\right)^*$$

$$\psi_0^2(\underline{x}) = \frac{1}{\sqrt{4\pi}}if_0(r)\sin\theta\exp(i\phi), \qquad \chi_{0\dot{2}}(\underline{x}) = -\psi_0^2(\underline{x})$$

A25

where θ, ϕ are angles in the "hidden" relative space $\underline{x}$.

Equations (A24-25) have been inserted into (A19) which has been converted into a first order system [4 (10.4.5)] that has been solved on a computer for the neutron, Σ^0 and Ξ^0 baryons. Here, the quark masses in §2.4 and the neutron mass have been used as input.

The unknown d_b constants in (A24) have been handled as follows. Firstly, d_{b4}=0 according to [4 (11.1.3)]. Once d_{b2} is chosen, the remaining d_{b1}, d_{b0} and d_b are uniquely fixed by computer solutions

satisfying the confinement boundary conditions $g_0(r{\to}\infty){\to}0$ and $f_0(r{\to}\infty){\to}0$. The set of constants with $d_{b2}=-0.3202$ GeV^5 given in [4 Table 11.1] turned out to predict the correct neutron decay time [4 Table 12.1] with the wave functions plotted in [4 Fig. 11.1b] or [6 Fig. 1]. Using these wave functions, the average diquark-quark *dd-u* distance has been evaluated to be 3.23 fm in [7 (2.5)]. A more detailed calculation adjusts it to 3.05 fm.

A6 Interquark interaction potentials in nucleon and meson

The associated strong interquark interaction potentials (A24, A22) for neutron with the above d_{b2} value are plotted in Fig. A1.
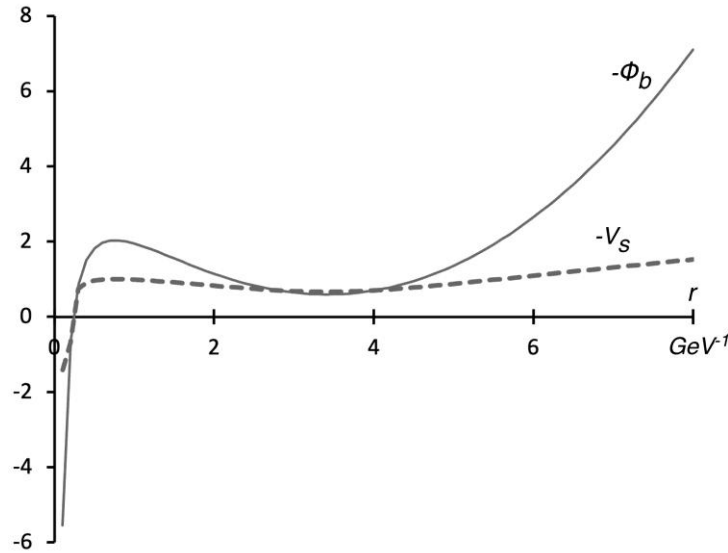

Fig. A1. Strong interaction potential Φ_b in units of GeV^3 in the equations of motion for neutron (A19) specified by (A24) with d_{b2}=−0.3202 GeV^5, d_{b1}=2.272 GeV^4, d_{b0}=−0.4.922 GeV^3, and d_{b0}=1.024GeV^5 [4 Table 11.1]. The *u-d* strong interaction potential $-V_s$ in units of GeV is inferred from (A22). The unit of *r* is GeV^{-1} = 1.24 fm

The equations of motion (A3) for quark *A* in nucleon, dropping the third quark *C* and gravitational terms, are the same as those in [4 (2.1.1)] for meson. Similarly, (A1) corresponds to the complex conjugate of the antiquark equations [4 (2.1.3)]. Thus, the *u-d* strong interaction potentials $V_{AB}(x_I)$ in (A3) and $V_{BA}(x_{II})$ in (A1) are the same as $V_{SB}(x_I)$ and $V_{SA}(x_{II})$, respectively, in [4 (2.1.1-4)], inasmuch as these are real and independent of complex conjugation. The intrameson strong interaction potential corresponding to Φ_b in (A14) is [4 (2.2.3)], which by analogy to (A22) becomes.

$$V_{SA}(x_{II})V_{SB}(x_I) \to \Phi_m(x_I, x_{II}) \to \Phi_m(r)$$

A26

The analog of (A24) in mesons is [4 (3.2.8a)], which by Table 5.2, (3.2.21) and (5.2.2) in [4] yields

$$\Phi_m(r) = d_{m0} + d_m/r + d_{m2}r^2 \to 0.64113 - 0.0049r^2 \text{ GeV}^2$$

A27

$$V_{sm}(r) = \mp\sqrt{\Phi_m(r)} = \mp\sqrt{0.64113 - 0.0049r^2} \approx \mp\left(0.8 - 0.0038r^2 - 7.3{\times}10^{-6}.r^4 ...\right) \text{ GeV}$$

A28

which corresponds to the interquark potential $V_s(r)$ in (A22) derived from the intranucleon *u-d* strong interaction. Comparison of $V_{sm}(r)$ to $V_s(r)$ in Fig. 2 show that both have the same magnitude of 0.67-0.9 GeV for $r \approx$ 1.6 - 5.1 GeV^{-1} or 2 - 6 fm where the bulk of the wave functions are concentrated (see

[6 Fig. 1] or [4 Fig. 11.1b)] and [4 (4.3.4a)]). The strengths of the strong interquark potentials in nucleon and meson are about the same and they support each other.

Here, it is noted that $V_{sm}(r)$ in (A28) has been determined from meson spectra in [4 Ch 5] and holds for any combination of a quark and an antiquark; the quark-quark strong interaction takes place in the hidden relative space and is flavor independent. Flavor dependent interactions include weak interactions, as have been considered in [4 Ch 7, 12].

A7 Upper limit of dark matter generation

The transformation constant a_m in (A16) can in principle be any real number and is related to the relative energy $-\omega$ in (A18). Negative $-\omega$ has been identified as dark matter in SSI [5 §5]. The ratio R_{DM} between the relative energy generated to the proton mass E_0, seen from (A18) and (A16) or (1) is [7 (4.2)],

$$R_{DM} = \frac{-\omega}{E_0} = -a_m + \frac{1}{2} = -\frac{|X - \underline{x}_I|}{|\underline{x}_{II} - \underline{x}_I|} + \frac{1}{2} = -\frac{X_p - x_I}{r_a} + \frac{1}{2} > -8.94$$

A29

Here, the distance between *uu* and *d*, $|\underline{x}_{II} - \underline{x}_I|$, has been approximated by its average value r_a = 3.23 fm in [7 (2.5)], which depends upon the wave functions $f_0(r)$ and $g_0(r)$ in (A25). A more detailed calculation modifies this value to r_a = 3.05 fm.

In [7 (4.2)], the quarks were heuristically required to lie inside the proton cloud having a radius of the proton Bohr radius a_{0p} = 28.8 fm. This requirement led to $|R_{DM}|$ < 8.4 there. With r_a = 3.05 fm, $|R_{DM}|$ < 8.94 in (A29).

A8 Proton viewed as a "*d-uu* rod"

As the quark masses in nucleon are nearly the same, the neutron results above can be taken over to apply for proton as well here.

The form of the interquark potentials $V_s(r)$ differs from those in earlier potential models [9] in that they are rather flat in the middle with a shallow minimum at $r \sim 4$ fm. This 4 fm is another average of the *u* to *d* distance and is of the same magnitude as the average r_a=3.05 fm mentioned in §**A7**. This distance in proton is fairly rigid due to the strong V_s bond. Thus, the "hidden" part of the proton may here be viewed phenomenologically as a *d-uu* aggregate bound by strong force Φ_b in Fig. A1 or a rigid "*d-uu* rod" of length 3.05 fm, with a *d* quark attached to one end and a *uu di*quark to the other. The mass of the three quarks in this rod is $2m_u + m_d$ = 1.97975 GeV. The rod itself may represent some average of the *u-d* attraction potential or strong bonding via $V_s \approx -1$ GeV in Fig. A1. The sum of these two energies yields the magnitude of the proton mass.